Sensors and Actuators B 144 (2010) 349–353

Contents lists available at ScienceDirect

Sensors and Actuators B: Chemical

journal homepage: www.elsevier.com/locate/snb

Mass transport effect of mesoscopic domains in the amperometric response of an electroactive species: Modeling for its applications in biomolecule detection

Graciela González, Graciela Priano, Mauricio Günther, Fernando Battaglini*

INQUIMAE - DQIAQF, Facultad de Ciencias Exactas y Naturales, Universidad de Buenos Aires, Ciudad Universitaria, Pabellón 2, 1428, Buenos Aires, Argentina

ARTICLE INFO

Article history:
Available online 19 November 2008

Keywords:
Mesoporous membrane
Digital simulation
Amperometry
Label-free sensing

ABSTRACT

We report the numerical simulation of an electrochemical system compromising a mesoporous material placed at a close distance of a working electrode. The effect of mesoscopic domains to the amperometric response of an electroactive species by applying a cyclic voltammetry is simulated to establish the influence of different parameters on the sensitivity of this system to detect molecules able to block the pores. Alumina membranes were chosen as mesoporous material; they were modified with anti-horseradish peroxidase as model system to test the behavior predicted by the simulation. The label-free assembled electrochemical system shows a reproducible behavior and it is able to detect a 10 nM protein concentration.

1. Introduction

In the last 15 years, important advances in the synthesis of mesoporous materials have made possible the development of very sensitive systems for molecule detection or ion channel investigations. Several systems have been reported in the literature, among them porous silicon [1–5], multipore membrane [6–10], single pore membrane [10–12] and more recently the glass nanopore electrode introduced by White et al., which combines, in the same device, a glass nanopore with a platinum or gold microelectrode [13]. These are label-free devices, since they can detect an analyte by simply using a common property to all molecules, its size. This fact, combined with the selective interaction through a recognition agent, can be useful to detect practically any molecule, providing the adequate size pore. Among the proposed solutions, single pore systems show a great sensitivity, potentially they can achieve single molecule detection; their response can also be easily modeled, however their experimental implementation is not so simple. On the other hand, even though multipore systems would not be able to carry out single molecule detection, they can achieve detection limits useful for a myriad of determinations. Among the multiporous membranes, alumina membranes present some advantages, they can be easily modified through a covalent link [6] or by a self-assembled process [14,15], pores in the size of biomolecules can be easily obtained and they are commercially available. On the other hand, they are fragile and models describing its possible behavior were not developed.

This work presents an electrochemical system that can be easily assembled, maintaining the integrity of the membrane and the reproducibility of results; at the same time a numerical tool was developed allowing the study of the system (electrochemical cell–porous membrane) identifying optimal parameters of operation. Finally, an experimental system compromising the modification of the alumina membrane with anti-horseradish peroxidase (anti-HRP) allows the detection of HRP as low as 10 nM.

2. Experimental and numerical system

2.1. Reagents and materials

Horseradish peroxidase (HRP) was provided by Biozyme, anti-horseradish peroxidase (anti-HRP), 3-aminopropyl(triethoxy) silane (APTES), 2-(N-morpholino)ethanesulfonic acid (MES), (4-(2-hydroxyethyl)-1-piperazineethanesulfonic acid (HEPES), N-(3-dimethylaminopropyl)-N′-ethylcarbodiimide hydrochloride (EDC) and N-hydroxysuccinimide (NHS) were provided by Sigma; alumina membranes, Anodisc 25, were provided by Whatman. All other reagents were of analytical grade.

2.2. Electrochemical cell

A two-part electrochemical cell made in Teflon was used. In the lower part, the working electrode is placed leaving a shallow cavity where a solution is introduced (Zone 1 in Scheme 1b). On the

* Corresponding author. Tel.: +54 11 45763380; fax: +54 11 45763341.
E-mail address: battagli@qi.fcen.uba.ar (F. Battaglini).

0925-4005/$ – see front matter © 2008 Elsevier B.V. All rights reserved.
doi:10.1016/j.snb.2008.11.006

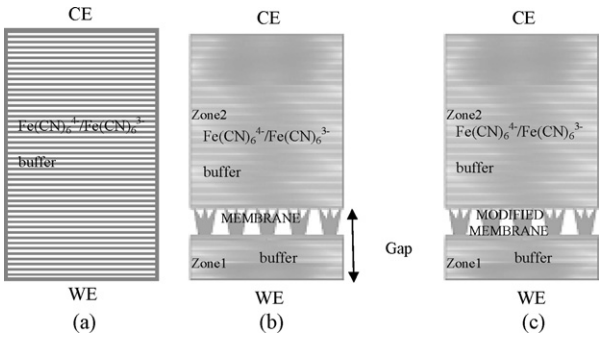

Scheme 1. Schematics (not on scale) of the cell configurations used in this work.

top of this part, an alumina membrane is placed. Over the alumina membrane the upper part of the cell is adjusted and filled with a solution (Zone 2 in Scheme 1b); then, the counter and Ag/AgCl reference electrodes are introduced.

2.3. Membrane modification

Alumina membranes were modified by two different ways: by partial insulation with an electrical insulating varnish (Electroquímica Delta, Argentina) and by covalent linking of anti-HRP. In this case, an alumina membrane was immersed in a 5% APTES solution in dry toluene under stirring for 1 h. The membrane is rinsed with toluene and placed in an oven at 120 °C for 20 min. Then, the membrane is placed in a 300 mM succinic anhydride solution in dimethyl sulfoxide (DMSO) under stirring overnight. The membrane is rinsed with DMSO, acetone and water. The surface is activated with a 100 mM EDC and 100 mM NHS in 50 mM MES buffer (pH 5.5) for 30 min under stirring, thereafter the surface is rinsed with water and incubated with a 1.8 mg mL^{-1} anti-horseradish peroxidase in 50 mM HEPES (pH 8.0) for 3 h under stirring. Then, the membrane is rinsed with water and the non-modified carboxylic groups were quenched with a 0.1 M ethanolamine solution (pH 8.5) for 15 min and then rinsed with water. The membrane is left in 0.1 M phosphate buffer (pH 7.4) for 10 min and rinsed. HRP is incubated at different concentrations in a 0.1 M phosphate buffer (pH 7.4) for 40 min, then, the membrane is rinsed with water.

2.4. Electrochemical experiments

Cyclic voltammetry experiments were carried out in a three electrode cell, using gold as working electrode at the base of the cell, in three different configurations (Scheme 1): (a) A standard three electrodes immersed in 2 mM $Fe(CN)_6^{3-}/Fe(CN)_6^{4-}$ solution containing 0.1 M supporting electrolyte in buffer pH 7; (b) In the presence of the porous alumina membrane placed at specific distance from the working electrode. The gap between the working electrode and the membrane is filled with buffer, while over the membrane, the cell is filled with the same solution than (a); and (c) the same as (b), with the membrane modified with an antibody (anti-HRP) or blocked with an insulating varnish.

2.5. Numerical model

This experimental system was modeled solving Poisson and Nernst–Plank without electroneutrality equations [16] using a finite-element software (Comsol Multiphysics 3.4) to obtain the voltammetric response and the concentration profiles, as previous works [13,17,18]. The space dimension was set to 2D and the boundary conditions were as an infinite plane electrode and semi-infinite diffusion. We employed a physical constant referred to the 2 mM $Fe(CN)_6^{3-}/Fe(CN)_6^{4-}$ redox couple in a solution containing 0.1 M supporting electrolyte. The flux of electroactive species at the electrode is given by

$$\frac{J_{\text{reac}}}{F} = \frac{J_0}{F}\left[\frac{C_R}{C_R^*}\exp\left(\frac{F}{2RT}\eta\right) - \frac{C_O}{C_O^*}\exp\left(-\frac{F}{2RT}\eta\right)\right] \quad (1)$$

where C_R^* and C_O^* are the concentration in the bulk solution, of the reduced and the oxidized species, respectively; C_R and C_O are the concentration on the working electrode surface of the reduced and the oxidized species, respectively; $\eta = E - E_{eq}$ is the applied overpotential and E_{eq} is the equilibrium electrode potential.

Table 1
Predicted peak current densities.

Sweep rate (mV s^{-1})	Theoretical	Numerical
50	563	549
100	796	757

Current densities in μA cm^{-2}.

2.6. Micrographs

Micrographs were taken with a field emission scanning electron microscope (FESEM) Zeiss DSM 982 Gemini at the Advanced Center for Microscopies (CMA, Universidad de Buenos Aires).

3. Results and discussion

Initially, the proposed simulation model was evaluated using a configuration without membrane (Scheme 1a) considering that the ferro/ferricyanide couple presents a quasireversible behavior. In this context, it is possible to compare the results obtained by the proposed simulation for the peak current density (j) with those predicted by the well established model published elsewhere [19]:

$$j_{p,qrev} = 6.02 \times 10^5 n^{3/2} D^{1/2} C^* \nu^{1/2} \Psi(E) \quad (2)$$

where $\Psi(E)$ is the quasireversible current function and can be considered 0.4 for a system like ferro/ferricyanide [19]; n is the number of electrons involved in the reaction; C^* is the bulk concentration of the electroactive species, D is the diffusion coefficient of the electroactive species and ν is the potential scan rate. Table 1 summarizes the peak current densities obtained using Eq. (2) and by the simulation procedure developed in this work, showing that it is able to generate an adequate solution.

Once, the simulation codes were validated, a model for the description of the experiments involving the introduction of a porous membrane was written (Scheme 1, cell configuration b). In this configuration, the electrochemical cell is divided in two by the introduction of the porous membrane. In the lower part of the cell is the working electrode, between the membrane and the working electrode is a shallow cavity filled with buffer, its effect was simulated considering a gap between 0 and 600 μm. On the other hand, in the upper part of the cell a solution of an electroactive species was considered. As the membrane is blocked (Scheme 1, configuration c), the passage of the electroactive species is more difficult, therefore the peak current is smaller.

In the simulation, the effect of the introduction of the membrane was taken into account using the information given by the membrane supplier (thickness: 60 μm, hole diameters: 20 and 200 nm, and porosity 25–50%) plus the structure information given by FESEM (Fig. 1). As it can be observed from the micrographs, the membranes have a very characteristic shape, the smaller pore size, at one side of the membrane (Fig. 1a), only extends for a few micrometers (Fig. 1c). Different geometries for the pore shape were considered, the one depicted in Scheme 1b shows the best fit with

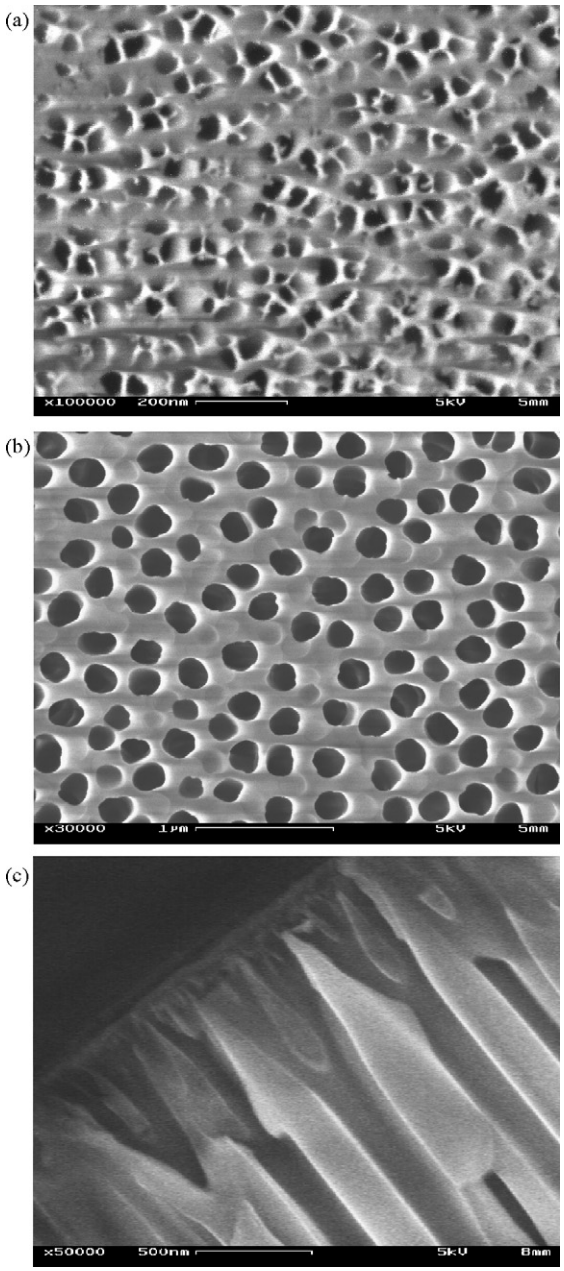

Fig. 1. FESEM images: (a) corresponding to the side oriented to the bulk solution (Zone 2 in Scheme 1b); (b) corresponding to the side oriented to the electrode (Zone 1 in Scheme 1b). (c) Membrane profile, the micrograph was taken close to the side oriented to the bulk solution.

the experimental results and it is a close representation of the used membrane.

Using Scheme 1, the effect of the distance between the working electrode and the membrane was tested considering the configuration b at three different distances, 0, 10 and 600 μm, corresponding to the gap marked in Scheme 1b. As the electroactive species has to diffuse from the membrane to the surface electrode, the allowed diffusion time set in the simulation is equivalent to the period needed to reach a surface concentration of 0.2–0.3 mM of the electroactive species, previous to the potential scanning. Fig. 2 shows the calculated cyclic voltammetries for the different cases, 600 μm (black line), 10 μm (light grey line), and onto the electrode (dark grey line). Even though, the three simulations start with the same concentration on the electrode surface, their concentration profiles present important differences, providing different fluxes of

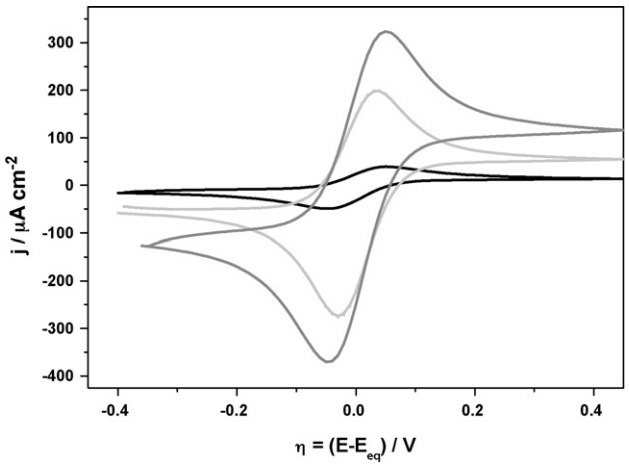

Fig. 2. Numerical simulation of the voltammetric response of 2 mM (1:1) $Fe(CN)_6^{3-}/Fe(CN)_6^{4-}$, 0.050 V/s with porous material placed at 600 μm (black line), 10 μm (light grey) and 0 μm (dark grey) from the working electrode.

the electroactive species as it is consumed at the electrodes surface; as the flux is smaller, the observed current is smaller. Fig. 3 depicts the concentration profiles for $Fe(CN)_6^{3-}$ at η equals to −0.10 V (dark grey) and at η equals to 0.45 V (light grey) at the three distances previously mentioned. Sharper concentration profiles for 0 and 10 μm gap can be observed with respect to the 600 μm gap, that explains the difference in the observed currents. The simulations establish that a small gap size between the working electrode and the membrane is an important condition to maintain the sensitivity of the signal. The most adequate condition would be to place the membrane onto the electrode surface. However, experimentally, this approach presents some problems regarding its reproducibility; small differences in the distance between the electrode surface and the membrane will bring in turn important differences in the observed current. This effect on the current response was studied using the numerical procedure presented here, its results are depicted in Fig. 4, it can be observed that at short working electrode–membrane distances, small changes can produce important changes in the current response. For this reason, an electrochemical cell in which the distance between the electrode surface and the membrane is 600 μm was designed; in this way small changes in the distance due to material deformations (less than 10 μm) would have practically no effect in the determinations.

The time left from the addition of the electroactive species in the Zone 2 (Scheme 1b) and the beginning of the cyclic voltammetry is other important aspect to take into account to develop a reproducible assay. Here, a trade off between the time to obtain a good signal and a reasonable waiting time, as small as possible, has to be found; in the present conditions 100 s was taken as waiting time before running a cyclic voltammetry.

Considering the previous parameters, the response to the diffusion of an electroactive species through a partially blocked membrane was studied by painting sections of the membrane with an insulating varnish; at the same time, its behavior was simulated. Fig. 5 shows experimental and numerical results obtained for a system compromising a blocked membrane at a 600 μm distance from the working electrode. The numerical data (diamonds) generated with the proposed model fits very well with the experimental results (squares). If the numerical data are plotted against the remaining free pores (inset in Fig. 5), two important features can be observed, first the trend of the current with the percentage of free pores present in the membrane perfectly fits a logarithmic behavior and, second as the number of free pores decreases the system becomes more sensitive. Other important aspect to mention on the conditions established for the reproducibility of this

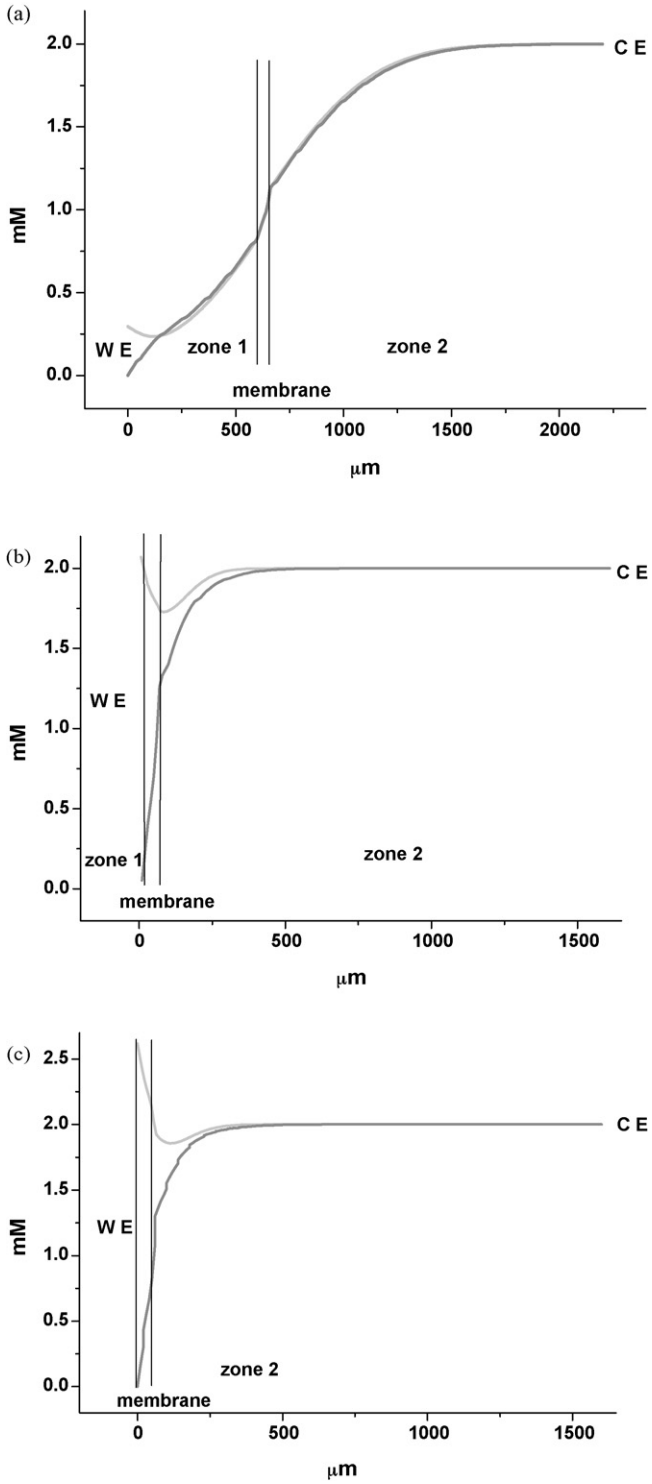

Fig. 3. Numerical quantitative concentration profiles of $Fe(CN)_6^{3-}$ at η equals to −0.10 V (dark grey) and 0.45 V (light grey), obtained from CV 2 mM (1:1) $Fe(CN)_6^{3-}/Fe(CN)_6^{4-}$, 0.05 V/s with porous material placed at (a) 600 μm, (b) 10 μm, and (c) 0 μm from the working electrode.

system is the fact the peak current were measured per duplicate in all the experimental points, assembling and disassembling the whole system and changing the membrane, showing differences between measurements less than 10%.

Finally, the alumina membrane was derivatized with APTES and further modified, through a covalent linkage, with anti-horseradish peroxidase. Fig. 6 shows the signal obtained for the modified membrane and when the membrane is incubated with 10 and 100 nM HRP solutions. These results indicate that the system is able to determine a concentration as low as 10 nM.

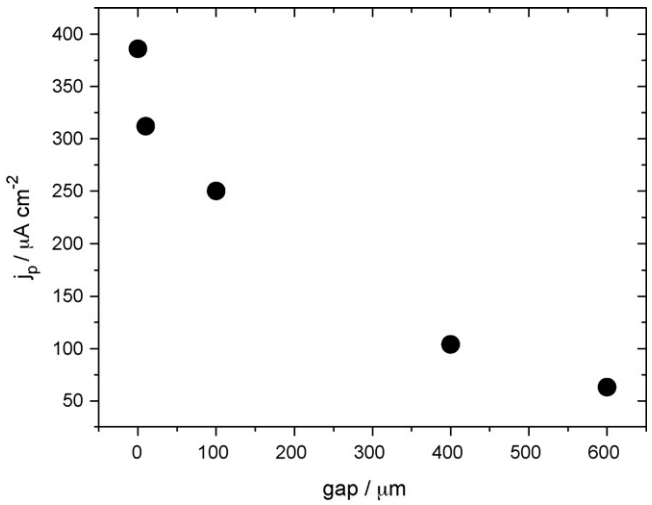

Fig. 4. Numerical amperometric response of 2 mM (1:1) $Fe(CN)_6^{3-}/Fe(CN)_6^{4-}$; sweep rate: 0.1 V/s using configuration B with the porous membrane placed at different gap distances from the working electrode.

In another set of experiments, higher concentrations of HRP were incubated to observe if a complete blockage of the membrane is possible. Fig. 7 shows (in solid line) the predicted behavior for the experimental conditions used as the pores are blocked. The black squares are the current densities obtained when the membrane was incubated at 100, 500 and 2000 nM. It can be observed that, even at very high HRP concentrations the system is not completely blocked. This can be attributed to the fact that HRP–anti-HRP complex as a whole must be smaller than 20 nm, taking into account their individual dimensions [20,21], while the pore size is ca. 20 nm; therefore, even though HRP introduces an obstacle to the passage of the small electroactive molecules, there are always some narrow free pathways, through which the probe reaches the working electrode.

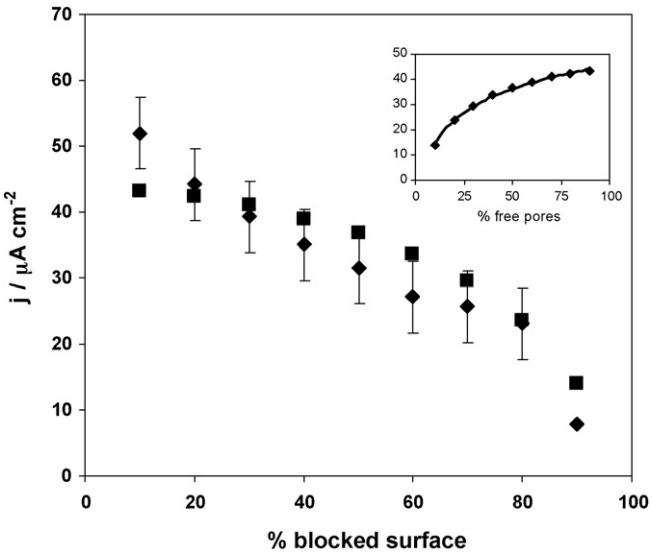

Fig. 5. Numerical and experimental amperometric response of a 2 mM (1:1) $Fe(CN)_6^{3}/Fe(CN)_6^{4-}$ solution obtained from cyclic voltammetry. Sweep rate: 0.05 V/s. Porous membrane placed at 600 μm from the working electrode. The inset shows the fitting of the calculated current with a logarithmic curve (r^2 = 0.997).

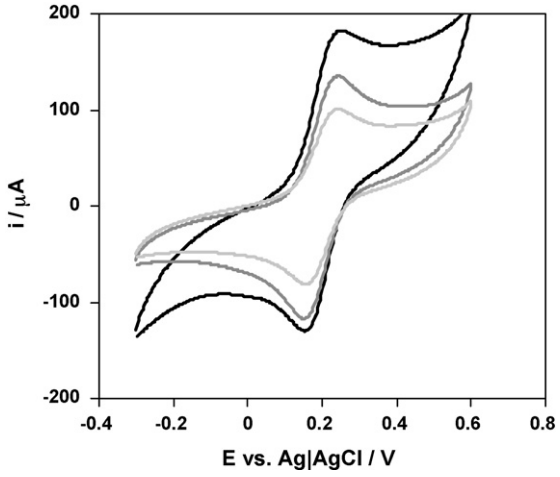

Fig. 6. Cyclic voltammetries for 2 mM (1:1) $Fe(CN)_6^{3-}/Fe(CN)_6^{4-}$, 0.1 V/s with the porous membrane modified with anti-HRP. The membrane was placed at 600 μm from the working electrode. Black line, response without HRP incubation; dark grey, response after incubation with 10 nM HRP; light grey, after incubation with 100 nM HRP.

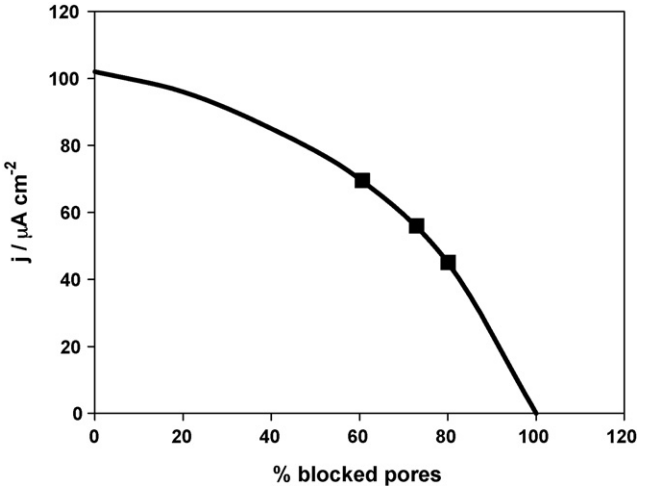

Fig. 7. Plot of the predicted current density (black line). Black squares are the current densities for membranes that were incubated with 100, 500 and 2000 nM HRP (decreasing currents).

4. Conclusions

The results presented here show that the mass transport in an electrochemical cell–porous membrane system can be described with the numerical and geometrical model proposed. The porous system combined with a very simple technique like cyclic voltammetry can be used as a sensitive tool for label-free detection of biomolecules. The experimental system built by the assistance of numerical simulations has demonstrated to behave in a reproducible way. Since the membrane is firmly enclosed in the electrochemical cell, its manipulation is facilitated avoiding the risk of accidental ruptures. Work is in progress to reduce the exposed membrane area and to use a more sensitive technique like square wave voltammetry. Finally, the fine tuning of the pore size is an important subject to be addressed if a specific application will be developed.

Acknowledgements

This work was supported by grants of Agencia de Promoción Científica (PICT 2006-00575) and Universidad de Buenos Aires (Project X012 and X850). Fernando Battaglini and Graciela González are research staff of CONICET.

References

[1] J.R. Link, M.J. Sailor, Smart dust: self-assembling, self-orienting photonic crystals of porous Si, PNAS 100 (2003) 10607–10610.
[2] R.C. Anderson, R.S. Muller, C.W. Tobias, Investigations of porous silicon for vapor sensing, Sens. Actuators A: Phys. 23 (1990) 835–839.
[3] M. Ben-Chorin, A. Kux, Adsorbate effects on photoluminescence and electrical conductivity of porous silicon, Appl. Phys. Lett. 64 (1994) 481–483.
[4] J.M. Lahuerhaas, M.J. Sailor, Chemical modification of the photoluminescence quenching of porous silicon, Science 261 (1993) 1567–1568.
[5] S. Chan, S. Horner, P. Fauchet, B.L. Miller, Identification of gram negative bacteria using nanoscale silicon microcavities, J. Am. Chem. Soc. 123 (2001) 11797–11798.
[6] I. Vlassiouk, P. Takmakov, S. Smirnov, Sensing DNA hybridization via ionic conductance through a nanoporous electrode, Langmuir 21 (2005) 4776–4778.
[7] H. Bayley, C.R. Martin, Resistive-pulse sensings from microbes to molecules, Chem. Rev. 100 (2000) 2575–2594.
[8] K. Nozawa, C. Osono, M. Sugawara, Biotinylated MCM-41 channels as a sensing element in planar bilayer lipid membranes, Sens. Actuators B: Chem. 126 (2007) 632–640.
[9] A. Mortari, A. Maaroof, D. Martin, M.B. Cortie, Mesoporous gold electrodes for sensors based on electrochemical double layer capacitance, Sens. Actuators B: Chem. 123 (2007) 262–268.
[10] Z. Siwy, L. Trofin, P. Kohli, L.A. Baker, C. Trautmann, C.R. Martin, Protein biosensors based on biofunctionalized conical gold nanotubes, J. Am. Chem. Soc. 127 (2005) 5000–5001.
[11] J.D. Uram, K. Ke, A.J. Hunt, M. Mayer, Label-free affinity assays by rapid detection of immune complexes in submicrometer pores, Angew. Chem. Int. Ed. 45 (2006) 2281–2285.
[12] T. Ito, L. Sun, R.R. Henriquez, R.M. Crooks, A carbon nanotube-based Coulter nanoparticle counter, Acc. Chem. Res. 37 (2004) 937–945.
[13] B. Zhang, Y.H. Zhang, H.S. White, The nanopore electrode, Anal. Chem. 76 (2004) 6229–6238.
[14] S.K. Kumar, J.-D. Hong, Photoresponsive ion gating function of an azobenzene polyelectrolyte multilayer spin-self-assembled on a nanoporous support, Langmuir 24 (2008) 4190–4193.
[15] S.U. Hong, M.L. Bruening, Separation of amino acid mixtures using multilayer polyelectrolyte nanofiltration membranes, J. Membr. Sci. 280 (2006) 1–5.
[16] J. Newman, K. Thomas-Alyea, Electrochemical Systems – Chapter 11, 3rd ed., John Wiley & Sons, 2004.
[17] Y.H. Zhang, B. Zhang, H.S. White, Electrochemistry of nanopore electrodes in low ionic strength solutions, J. Phys. Chem. B 110 (2006) 1768–1774.
[18] S. Lee, Y. Zhang, H.S. White, C.C. Harrell, C.R. Martin, Electrophoretic capture and detection of nanoparticles at the opening of a membrane pore using scanning electrochemical microscopy, Anal. Chem. 76 (2004) 6108–6115.
[19] A.J. Bard, L.R. Faulkner, Electrochemical Methods, 2nd ed., Wiley, New York, 2001, Chapter 6, pp. 236–239.
[20] G.I. Berglund, G.H. Carlsson, A.T. Smith, H. Szoke, A. Henriksen, J. Hajdu, The catalytic pathway of horseradish peroxidase at high resolution, Nature 417 (2002) 463–468.
[21] G. Demirel, T. Çaykara, B. Akaoglu, M. Çakmak, Construction of a novel multilayer system and its use for oriented immobilization of immunoglobulin G, Surf. Sci. 601 (2007) 4563–4570.

Biographies

Graciela Alicia González is a Lecturer at Universidad de Buenos Aires and research staff of the Argentina Research Council (CONICET). She received her PhD from Universidad de Buenos Aires (2003). Her research interests are modeling of electrochemical processes, nanotechnology and materials science.

Graciela Priano is a researcher at Facultad de Ciencias Exactas y Naturales, Universidad de Buenos Aires, Argentina. She obtained her Licenciatura en Ciencias Químicas at the same University, where she also received her PhD in Chemistry (2006). Her work focuses on the functionalization of surfaces with specific recognition molecules for the development of test and sensors applied to endotoxin detection. She also works on its application on silicon porous structures in collaboration with Dr. R. Koropecki's Group (Universidad del Litoral, Argentina).

Mauricio Günther is an undergraduate and fellow student of chemistry at Universidad de Buenos Aires.

Fernando Battaglini is an Associate Professor at Universidad de Buenos Aires and research staff of the Argentina Research Council (CONICET). He received his PhD from Universidad de Buenos Aires in 1991. His research interests are biosensors, electrochemistry and materials science.